

The solution structure of the intramolecular photoproduct of d(TpA) derived with the use of NMR and a combination of distance geometry and molecular dynamics

T.M.G.Koning, R.J.H.Davies[1] and R.Kaptein
Department of Chemistry, University of Utrecht, Padualaan 8, 3584 CH Utrecht, The Netherlands and [1]Biochemistry Department, Medical Biology Centre, Queen's University, Belfast BT9 7BL, UK

Received October 5, 1989; Revised and Accepted December 14, 1989

ABSTRACT

One and two dimensional NMR techniques have been used together with molecular modelling to obtain the solution structure for the photoproduct d(TpA)*. The NMR data confirm that the cyclobutane linkage is formed between the bonds thymine C6-C5 and adenine C5-C6. The 2D NOE data are used as constraints in a distance geometry calculation. The structures obtained show a *trans-syn* cyclobutane linkage and the glycosidic angles are SYN and ANTI for thymidine and deoxyadenosine, respectively. The coupling constant data are used to check the backbone torsion angles of the obtained structures. Typical torsion angles are a γ^+ and β^t for the deoxyadenosine residue. A free molecular dynamics simulation of a *trans-syn* d(TpA) photoproduct confirmed all these structural characteristics.

INTRODUCTION

Much of the biological damage sustained by living cells exposed to short wavelength ultraviolet (UV) light originates from photochemical reactions of the nucleobases within their DNA and the ensuing mutational events (*1*). Generally, however, the relationship between a given photolesion and the resulting mutations is poorly understood. In elucidating this connection, it is important to define the perturbations to the structure of DNA which accompany the formation of specific photoproducts and thereby gain insight into how they influence the molecular recognition processes which govern the replication, transcription and repair of DNA. The main photoproducts formed in DNA comprise *cis-syn* cyclobutane pyrimidine dimers and bipyrimidine (6−4) photoadducts (*1*). Several accounts have been published (*2−10*) where high resolution NMR spectroscopy has been used to determine the structures of these photolesions when they are incorporated into deoxydinucleoside monophosphates or longer oligonucleotides in solution.

The purine components of DNA are considerably more resistant towards photochemical alteration than their pyrimidine counterparts. Nonetheless, photodimerization of adjacent adenines occurs quite readily in d(ApA) and higher polymers of deoxyadenylic acid (*11,12*). Adjacent thymine and adenine bases in d(TpA) units also undergo an intramolecular photoaddition reaction on irradiation at 254 nm in solution (*13*). The resulting thymine-adenine photoadduct has been detected in UV-irradiated DNA as well as in oligo- and poly(dA-dT). The quantum yield for its formation ranges from about 7×10^{-4} mole/E in the deoxydinucleoside monophosphate to 1×10^{-5} mole/E in native calf thymus DNA (*13*); the photoreaction is strongly quenched by base pairing.

In this paper, we report an NMR study of the intramolecular photoproduct prepared from d(TpA) whose chemical characterization has been described elsewhere (*14*). A schematic representation of the molecule, which is herein referred to as d(TpA)*, is shown in Figure 1; the nomenclature for the torsion angles is also indicated in the figure. Proton-proton distances derived from 2D NOE data are used as constraints in a distance geometry calculation. The structure of the photoproduct derived in this way has a *trans-syn* cyclobutane linkage between the thymine and adenine bases. The glycosidic angles for the thymidine and deoxyadenosine moieties are found to be in the SYN and ANTI regions respectively. The coupling constants of the molecule have been measured and they provide evidence for an extended phosphate backbone geometry. The NMR results and the structure will be discussed in detail. Finally the results of a free molecular dynamics simulation of *trans-syn* d(TpA)* will be presented.

MATERIALS AND METHODS

The photoproduct d(TpA)* was generated by irradiating d(TpA) in neutral aqueous solution at 254 nm according to Bose et al (*14*) and then isolated by a more convenient procedure utilizing high performance liquid chromatography (HPLC) with equipment described in reference 12. The UV irradiated solution of d(TpA) was lyophilized and the residue redissolved in distilled water at a concentration of ~ 20 mg ml^{-1}. Aliquots of this solution (100−200 μl) were injected onto a semi-preparative column (300×7.8 mm) of μ Bondapak C_{18} (Waters Associates) which was eluted, at a flow rate of 3.0 ml min^{-1}, isocratically with water for 5 min followed by a linear gradient to 30% aqueous methanol after 15 min and isocratic elution with this mixture for a further 10 min. The elution profile, monitored at 254 nm, showed two well separated major peaks at 4.5 min and 16 min, corresponding to d(TpA)* and unchanged d(TpA) respectively,

together with a number of minor peaks. Fractions comprising the d(TpA)* peak were pooled, lyophilized and then repurified by repeating the HPLC fractionation once more. The d(TpA)* thus obtained (in an overall yield of ~ 25%) gave a single sharp peak on analytical HPLC and exhibited the same UV spectrum as reported previously (*13*). For NMR measurements, samples of d(TpA)* were lyophilized twice from D_2O and then dissolved in a buffer (50 mM KP_i and 200 mM NaCl, pD 6.55) to give a final concentration of 2mM.

NMR spectra were taken on a Bruker AM 500 spectrometer. For the ^{31}P decoupled spectra a WALTZ scheme(*15*) was used for decoupling. Two dimensional COSY and NOESY spectra were recorded as described elsewhere (*16,17*). For the phase-sensitive 2D NOE spectrum 512 FID's of 2048 data points were collected with a spectral width of 5000 Hz. The relaxation delay was 4 s and a mixing time of 0.75 s was used. The data were processed on a μVAX 2 with the '2D NMR' software package written in Fortran 77. In the t_2 dimension the data points are multiplied with a $\pi/2$ shifted sine bell. In the t_1 dimension the same window function was used and the data were zero filled once before Fourier transformation. After the two-dimensional Fourier transformation the spectrum was baseline corrected in the ω_1 dimension. The final resolution of the 2D NOE spectrum was 5 Hz/point. In the case of the COSY experiment the time domains were multiplied by a sine bell shifted ($\pi/3$) before absolute value Fourier transformation. Pseudorotational analysis of the furanose ring based on the ^1H- ^1H coupling constants was carried out using a method developed by Haasnoot et al.(*18,19*).

Three dimensional structures were generated using the distance geometry program DG derived from the original EMBED program (*20*). First the distance matrix was smoothed using the triangle inequalities. After this the structures were embedded in three dimensions and finally 300 steps of optimization were performed using an error function which included distance and chirality constraints. The distance bound driven dynamics algorithm (DDD) was applied for 1000 steps at 300K and 300 steps at 1K (*21*).

For the energy minimization and molecular dynamics simulation the GROMOS force field and programs were used (*22,23*). In a restrained steepest descent energy minimization the force constant for the distance constraints was 4000 kJ/mole.nm^2. Typically 100 to 200 steps were necessary until the energy of the structures did not change any more and the gradient was sufficiently low. For the free molecular dynamics simulation one of the DG structures was put in a rectangular box with 212 water molecules and one sodium ion. The inital velocities were taken from a Maxwellian distribution at 300 K. Throughout the simulation periodic boundary conditions were applied and the system was coupled to an external bath of 300 K. The simulation was over a period of 30 ps and the trajectories of the last 20 ps were used for averaging and analysis.

RESULTS AND DISCUSSION

NMR assignments

The assignment of the resonance positions of the protons in the deoxyribose spin systems was accomplished using the COSY experiment. The ^1H 500 MHz spectrum, which is shown in Figure 2, together with the ^{31}P decoupled spectrum have been used to identify these spin-systems.The spin system at the 5'-end, belonging to thymidine, contains a H3' proton which is coupled to the phosphorus, whereas for the 3'-end sugar ring this is the

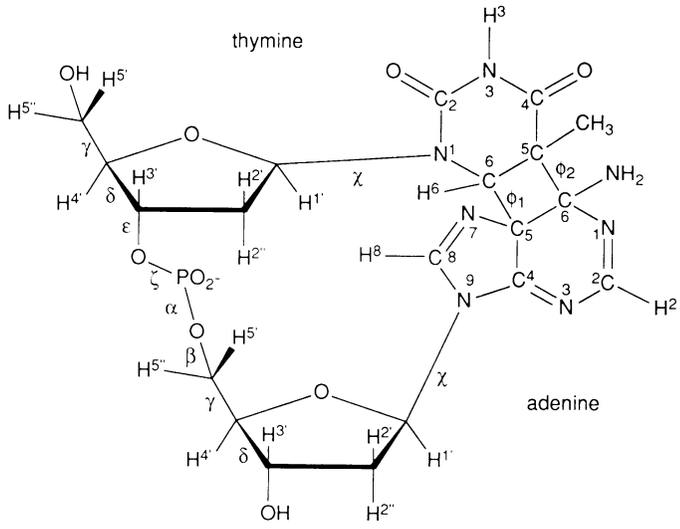

Figure 1. Schematic presentation of the cyclobutane photoproduct of d(TpA). The standard numbering for the bases and the deoxyribose is shown and the names of the torsion angles are indicated.

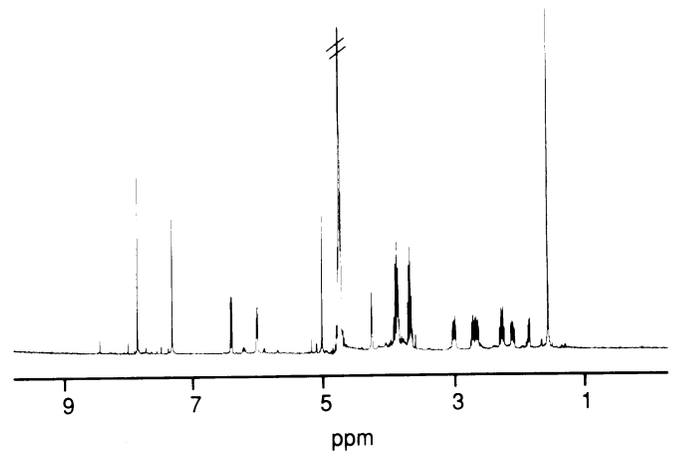

Figure 2. ^1H 500 MHz NMR spectrum of d(TpA)* in D_2O (50 mM KP_i, 200 mM NaCl, pD = 6.55, 300 K). The chemical shifts are relative to DSS.

case for the H5' and H5'' protons. In this way the spin systems were specifically assigned very easily.

In the 2D NOESY spectrum, shown in Figure 3, for the adenine H2 proton (δ=7.28 ppm) no cross peaks were observed. This proton resides at a site of the molecule where no other non-exchangeable protons are nearby. The methyl group (δ=1.58 ppm) has a strong cross peak with the base proton H6 (δ=5.03 ppm) of thymine. Therefore the only unassigned resonance position left has to be the adenine H8 (δ=7.83 ppm). The assignments are indicated in the 2D NOE spectrum in Figure 3 and the chemical shifts for all the protons are listed in Table 1.

Bose et al. (*14*) provided evidence that the covalent link between the two bases is formed between the atoms C5 and C6 of thymine and C6 and C5 of adenine (c.f. Figure 1). The chemical shifts of the base protons are in accordance with this. The H6 of thymine shifts to higher field because of saturation of the pyrimidine ring at the C5-C6 bond. Furthermore, the protons H8 and H2 resonate in the aromatic part of the spectrum. This is in agreement with the finding that the C8 and C2 atoms are not involved in cyclobutane ring formation.

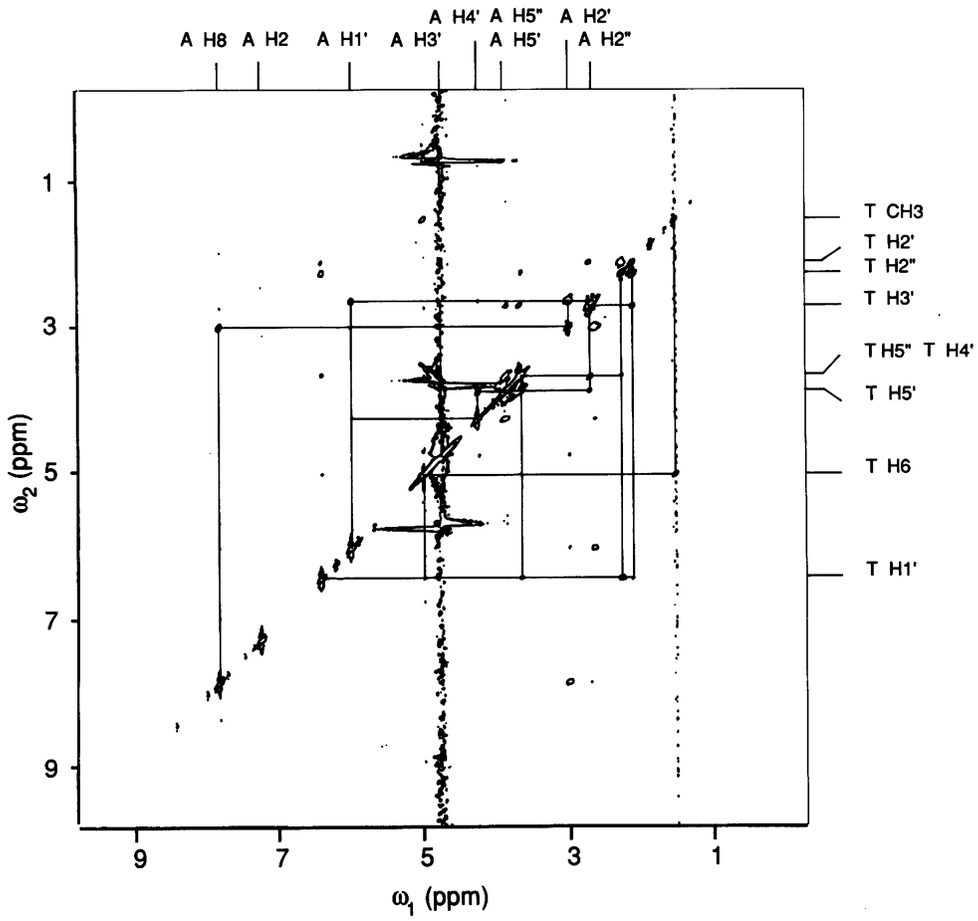

Figure 3. 500 MHz 2D NOE spectrum of d(TpA)* at 300 K. The mixing time is 0.75 s. The cross peaks have a negative sign, whereas the diagonal peaks have a positive sign. Below the diagonal the connectivities observed for the thymidine residue are indicated and above the diagonal those for deoxyadenosine.

Apart from the large shift of the H6 proton of thymidine the H3′ proton of this residue also exhibits a large upfield shift, $\Delta\delta = -1.86$ ppm, when compared to its chemical shift in the native dTpA (*24*). A possible explanation for this is the presence of an anisotropic group at a very short distance of this proton. When the pucker of the deoxyribose ring is in the C3′-endo region and the glycosidic angle χ is around 90° the carboxyl group of thymine is very close to the H3′ proton. Calculations have shown that the upfield shift of the H3′ proton can be more than −1.5 ppm in this case (*25*).

Analysis of the coupling constants

The high resolution ^{1}H 500 MHz spectrum in comparison with the ^{31}P decoupled spectrum has been used for the determination of the ^{1}H- ^{1}H couplings and the ^{1}H- ^{31}P couplings. Simulation of the spectra leads to a very accurate determination of the coupling constants, which are listed in Table 2.

The coupling constants of the sugar protons H1′ to H4′ are interpreted in terms of Φ (phase angle of pseudorotation), P(amplitude) and population of the S-type conformer (*18,19*). For thymidine the calculated values for the pseudorotation parameters are P=42° and Φ=35°, indicating a preference for the N-type, C3′-endo-C4′-exo, sugar conformation. This preference for the N-type sugar pucker is in accordance with the large shift of the thymidine H3′ proton. The deoxyadenosine sugar ring exhibits a preference for the C3′-exo conformation, P=198° and Φ=39°. However, both sugars are not conformationally pure since the values for population of the S-type conformers are 55% and 49% for thymidine and deoxyadenosine respectively.

Table 1. ^{1}H chemical shifts of the protons of the photoproduct d(TpA)* in ppm relative to DSS at 300 K.

proton	dTp[]-	-p[]dA
H1′	6.40	6.01
H2′	2.12	3.01
H2″	2.28	2.67
H3′	2.73	4.79
H4′	3.67	4.26
H5′[a]	3.87	3.86
H5″[a]	3.70	3.86
H6 / H8	5.03	7.83
Me5 / H2	1.58	7.28

[a] The H5′ and H5″ were assigned only pairwise.

The coupling data in the H4′, H5′ and H5″ region provide information about the phosphate backbone of the molecule. The torsion angle γ (O5′-C5′-C4′-C3′) is monitored through the proton-proton coupling constants $J_{4'5'}$ and $J_{4'5''}$. The population of the γ^+ rotamer can be calculated by means of an approximate sum rule from the sum of the $J_{4'5'}$ and $J_{4'5''}$ couplings (Σ) (*26*):

$$p\,\gamma^+ = (13.7-\Sigma) / 9.7$$

Table 2. Observed coupling constants (in Hz) for the deoxyribose moieties of d(TpA)* .

Coupling constant	dTp[]-	-p[]dA
$J_{1'2'}$	2.7	4.6
$J_{1'2''}$	9.7	6.8
$J_{2'3'}$	8.3	6.1
$J_{2''3'}$	9.6	5.3
$J_{3'4'}$	8.1	4.0
$J_{4'5'}$[a]	3.0	2.3
$J_{4'5''}$[a]	6.5	2.0
$J_{3'P}$	7.5	–
$J_{4'P}$	–	3.5
$J_{5'P}$[a]	–	2.3
$J_{5''P}$[a]	–	2.3

[a] The H5′ and H5″ were assigned only pairwise.

Table 3. The distance constraints as used in the distance geometry calculation and energy minimization.

	NOEs	distance (Å)
Thy H6 –	Thy C5 methyl	<3.0
Thy H1′ –	Thy H6	<3.5
Thy H1′ –	Thy H2″	<2.5
Thy H1′ –	Thy H2′	<3.5
Thy H4′ –	Thy H3′	<3.0
Thy H2′ –	Thy H3′	<2.5
Ade H8 –	Ade H2′	<2.5
Ade H8 –	Ade H2″	<3.5
Ade H1′ –	Ade H2″	<2.5
Ade H1′ –	Ade H2′	<3.5
Ade H1′ –	Ade H3′	<3.5
Ade H4′ –	Ade H3′	<2.5
Ade H2″ –	Ade H3′	<3.5
	non NOEs:	
Thy H6 –	Thy H2′	>3.5
Thy H6 –	Thy H2″	>3.5
Ade H8 –	Ade H1′	>3.5

Table 4. The root mean square deviations (Å) of the five d(TpA)* structures[a].

Structure	1	2	3	4	5
1	–	0.94	1.57	0.45	1.14
2	0.47	–	1.76	0.95	0.91
3	0.65	0.51	–	1.47	1.71
4	0.31	0.36	0.71	–	1.19
5	0.76	0.65	0.31	0.84	–

[a] Above the diagonal for the structures obtained after distance geometry, below the diagonal for the structures after distance bound driven dynamics.

The value of the population for the γ^+ rotamer, p γ^+ = 48%, indicates that there is a large conformational freedom for rotation about this bond in the thymidine. For the deoxyadenosine, however, there is a strong preference for the γ^+ rotamer, p γ^+ = 98%.

The torsion angle β (P-O5′-C5′-C4′) is monitored by the sum of the coupling constants $J_{P5'}$ and $J_{P5''}$ (Σ') via (*26*):

$$p\,(gg) = (25-\Sigma) / 20.8$$

Application of this sum rule indicates that the torsion angle β has a trans conformation with a high occupancy of 98%. For deoxyadenosine both β and γ show a large preference for the gauche-gauche arrangment. As a consequence the H4′ and P lie in an in-plane W-path and the long range four bond coupling $J_{4'P}$ is indeed observable, $J_{4'P}$=3.5 Hz, as expected.

There is still another backbone torsion angle conformation which can be determined. From the H3′-^{31}P coupling the torsion angle ϵ (H3′-C3′-O3′-P) can be calculated using the Karplus relation proposed by Lankhorst et al. (*27*):

$$J_{3'P} = 15.3\cos^2\phi - 6.1\cos\phi + 1.6$$

This leads to a value of 152° for this torsion angle ϵ.

For the backbone angles α and ζ nothing can be said using only the ^{1}H- ^{1}H and ^{1}H-^{31}P coupling constant data.

2D NOE spectroscopy

The 2D NOE spectrum of d(TpA)* shown in Figure 3 was used for assignment. Apart from this the NOE cross peaks give structural information because the dipolar interaction between proton pairs which are close in space is monitored. Since the dinucleoside monophosphate is in the fast tumbling limit the NOE cross peaks arise only due to direct magnetization transfer, i.e. there is no spin diffusion. Therefore only a few cross peaks can be observed between proton pairs which are at a distance up to about 3.5 Å.

An important structural aspect of this system is the conformation about the glycosidic bond (torsion angle χ). If this conformation is ANTI as it is for most of the A- and B- DNA duplexes, the base protons (H6 or H8) are close to the H2′, whereas the H1′ proton is pointing in the other direction and is far from the base protons. On the other hand, if the glycosidic bond is SYN, the situation is reversed. The H1′ proton is close to the base proton and the H2′ and H2″ protons are pointing away (*28*). Inspecting the NOE patterns for the base protons of thymidine and deoxyadenosine, we find for thymidine that there is a weak cross peak between the H6 base proton and the H1′ and furthermore the cross peaks between the H6 and the H2′ and H2″ are lacking. Therefore the glycosidic angle of the thymidine moiety is in the SYN range. Considering the cross-peak pattern for the adenine base proton H8, there are strong peaks between the H8 and the H2′and H2″ and no cross peak to the H1′ and hence the conformation around this glycosidic bond is ANTI.

Structure generation and refinement

The constraints which are used in the distance geometry calculation are listed in Table 3. The observed NOEs have been divided, somewhat arbitrarily, into three classes: strong, corresponding with a distance less than 2.5 Å, medium, less than 3.0 Å and weak, less than 3.5 Å. Also, the absence of NOEs, called non-NOEs, is used at this stage. The non-NOEs for thymidine H6-H2′ and H6-H2″ and for deoxyadenosine H8-H1′ were put in as constraints with a lower distance bound of 3.5 Å. This was done in order to restrain the χ angles to the SYN-ANTI conformations. Furthermore, two additional constraints took account of the covalent link between the two bases. Both interbase C5-C6 bonds were constrained to a value of 1.65 Å. Free rotation was permitted about the thymine C6-C5 and adenine C6-C5 bonds, in order to allow puckering of the cyclobutane ring.

No coupling data were included as constraints because only for the backbone torsion angles β and γ of deoxyadenosine could the data be assigned unambiguously to a unique conformation. In all the other cases they indicate the presence of conformational

Table 5. The potential energy (E-pot) and the distance restraint energy (E-dr) of the five finally derived structures before and after energy minimization.

	before		after	
structure	E-pot (kJ/mole)	E-dr (kJ/mole)	E-pot (kJ/mole)	E-dr (kJ/mole)
1	192	0.2	−45.3	0.3
2	175	0.5	−74.8	0.3
3	291	0.8	−30.4	0.4
4	223	0.2	−54.2	0.4
5	272	0.3	−18.3	0.2

equilibria in the molecule. These coupling data are used as a check on the models finally obtained for the d(TpA)* structure.

The distance matrix, containing upper and lower distance bounds for the distance geometry calculation, was calculated using the covalent structure of a d(TpA) molecule and the constraints as listed in Table 3. Using this matrix a set of 16 different structures was embedded and optimized. As described, different types of optimization were used. The first uses only an error function of distance bounds and chiralities. The second step, the distance bound driven dynamics, has the advantage that a larger part of the conformational space consistent with the distance bounds is searched due to the kinetic energy of the system (*21*).

The five best structures, in terms of distance violations, were selected and analysed. In Table 4 the root mean square deviations (rmsd) between the coordinates in the different structures are listed both before and after the application of the DDD algorithm. The flexible 5′-end, the hydroxyl group and the C5′ with its protons attached to it, were left out of the calculation of the rmsd values. After DDD the structures showed fewer distance violations. The rmsd values were also smaller, which is contrary to experiences with proteins (*21*). Apparently, the initial set of structures already samples the allowed conformational space quite well.

The final stage of structure refinement included potential energy terms in addition to the distance constraints. All five structures have been energy minimized using the GROMOS force field (*22,23*) for restrained EM. For all structures the initial total potential energy is quite high, whereas the distance constraints energy is almost zero. The total potential energy drops down very quickly and the distance constraints energy remains close to zero. The values for the potential energy and the distance constraints energy before and after EM are listed in Table 5. There are no major differences between the structures in terms of total potential energy.

Since not all the possible non-NOEs were included in the structure generation the final structures were also checked against these. Based on a lower bound distance of 3.5 Å the only violation which was detected was the contact between the thymidine H1′ and the adenine H8, for two of the structures (average violation 0.3 Å). All the other non-NOE observations were satisfied by the structures.

The rmsd for the five structures after restrained EM are calculated again and listed in Table 6. The spread in rmsd values is comparable with the spread in Table 4, so we can conclude that the restrained EM does not invoke large structural changes in the models. The average rmsd value for the five structures is 0.53 Å. The set of five structures is shown in Figure 4.

Analysis of the structures

Conformation about the cyclobutane ring.

The two bases linked by the cyclobutane ring can adopt two different configurations, when they are also linked through the phosphate backbone as in dinucleotides and DNA (*2*). The first one where the thymine and the adenine rings are located on the same side of the cyclobutane ring is called the *cis-syn* configuration. In the *trans-syn* configuration the thymine and adenine bases reside on opposite sides of the ring. The torsion angles ϕ_1 (T:N1-T:C6-A:C5-A:C4) and ϕ_2 (T:C4-T:C5-A:C6-A:N1) have values around zero in a *cis-syn* and about 180° in a *trans-syn* configuration. It is clear from the values ϕ_1 and ϕ_2 in Table 7 that in all five structures the cyclobutane linkage is in the *trans-syn* family.

Table 6. The root mean square deviations (Å) of the five d(TpA)* structures, obtained after distance geometry distance bound driven dynamics and energy minimization

Structure	1	2	3	4	5
1	–	0.50	0.57	0.42	0.63
2		–	0.54	0.30	0.65
3			–	0.69	0.28
4				–	0.78
5					–

Conformation about the glycosidic bond.

As can be seen in Table 7 the values for the glycosidic angle of thymidine range from 90° to 165°, corresponding with a SYN conformation. These values agree with the value of 90° which was predicted on the basis of the large shift of the thymidine H3′ proton. For deoxyadenosine all the glycosidic angles are in an ANTI conformation, ranging from −74° to −100°. These findings are in agreement with previous results on TpT (*5*) where a SYN-ANTI glycosidic pattern was found for a *trans-syn* photodimer.

Analysis of the torsion angles.

Starting at the 5′-end of the dinucleotide the first torsion angle is the γ of thymidine. As shown in Table 7 large variations in the value of this torsion angle can be observed. This corresponds with the analysis of the coupling constant data where it was found that this dihedral is not conformationally pure.

The torsion angle γ of deoxyadenosine should adopt a γ^+ conformation on the basis of the coupling data and this conformer was found for all but one structure. The torsion angle γ of structure 1 adopts a trans conformation.

On the basis of the coupling constant data the torsion angle β of deoxyadenosine could be determined to have a pure β^t conformation. In Table 7 it can be seen that for all the structures the angle β is indeed around 180°. It can be concluded that there is good agreement for these backbone torsion angles between the values calculated from the coupling constants and those found in the NOE-based structures.

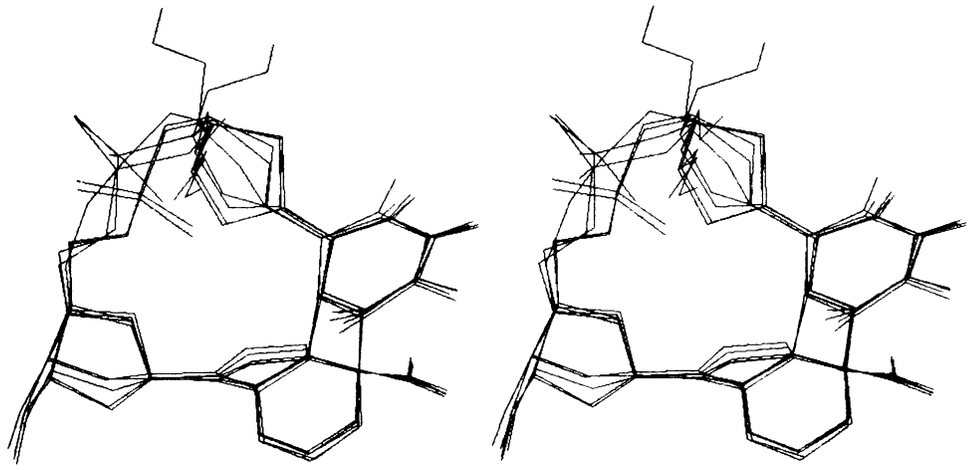

Figure 4. Stereoview of the set of five solution structures for d(TpA)*.

Table 7. The torsion angles (in degrees) for the d(TpA)* structures obtained after distance geometry, distance bound driven dynamics and energy minimization.

structure torsion angle	1	2	3	4	5
1 γ	−167	166	54	−179	−124
1 δ	144	165	134	168	115
1 χ	162	148	135	165	90
1 ϵ	33	−53	68	−44	80
1 ζ	−45	87	−45	75	−50
2 α	153	−127	−94	−165	−103
2 β	−145	172	−147	151	−143
2 γ	176	73	82	125	89
2 δ	154	146	151	144	156
2 χ	−100	−83	−74	−98	−82
ϕ_1	129	123	120	127	122
ϕ_2	−103	−108	−113	−104	−109

The torsion angles δ are directly related to the sugar pucker. In all five structures the values for δ correspond with a S-type geometry for both deoxyribose units, whereas on basis of the coupling constant data equilibria between N- and S-type sugar conformations were expected.

The value of the torsion angle ϵ was expected to be 152° on the basis of the value of the coupling constant between H3′ and ^{31}P. As shown in Table 7 the value for this torsion angle deviates from this expected value and shows a large variation. Probably, there are a number of possible conformations for this part of the phosphate backbone.

Although the match between this set of models and the NMR parameters is quite good, the question arises whether other types of photodimers are also consistent with the data. The only other possible structure would be the *cis-syn* cyclobutane linkage since the other *trans-syn* structure does not fit the SYN-ANTI glycosidic angle pattern. In the case of the *cis-syn* cyclobutane dimer of d(TpT) this pattern was indeed observed, both in solution and in the crystal structure (*8,29*). However, modelling of the d(TpA)* into the *cis-syn* conformation yielded structures with higher energy and larger violations of the NMR constraints.

Free molecular dynamics simulation

Since it would be interesting to see how the generated structures behave when the constraints are switched off, we have taken the structure with the lowest energy, structure 2, as starting structure for a free molecular dynamics simulation including solvent and a counterion. A trajectory of 20 ps and the average structure were analysed in the same way as the DG and DDD structures.

Table 8. The average torsion angles and the fluctuations in these angles (in degrees) for the 20 ps trajectory of the free molecular dynamics simulation of d(TpA)*

torsion angles	average	fluctuation
1 γ	−169	17
1 δ	116	23
1 χ	28	20
1 ϵ	198	13
1 ζ	−88	18
2 α	−106	41
2 β	174	26
2 γ	58	11
2 δ	127	19
2 χ	−53	28
ϕ_1	108	13
ϕ_2	−122	12

The average MD structure shows a minor structural change compared to the starting structure. This is reflected in the rmsd of the coordinates of the average structure and the starting structure, which at 1.14 Å is somewhat higher than the positional fluctuation of the atoms (0.64 Å).

In Table 8 the behavior of the torsion angles during the run is shown. From this table it is clear that all the torsion angles have about the same values as the set of generated structures.

Table 9. The average distances (Å) between the proton pairs during the 20 ps trajectories of the free molecular dynamics simulation of d(TpA)* and the constraints which were used to build the models.

proton pair	average distance	constraint	proton pair	average distance	constraint
T H6 – T Me	3.10	<3.0	A H1′ – A H2″	2.38	<2.5
T H6 – T H1′	2.64	<3.5	A H1′ – A H3′	3.83	<3.5
T H1′ – T H2″	2.45	<2.5	A H3′ – A H4′	2.83	<2.5
T H1′ – T H2′	3.08	<3.5	A H3′ – A H2″	2.78	<3.5
T H3′ – T H4′	2.94	<3.0	T H6 – T H2″	3.90	>3.5
A H8 – A H2″	2.99	<3.5	T H6 – T H2″	3.21	>3.5
A H8 – A H2′	2.59	<2.5	A H8 – A H1′	3.42	>3.5
A H1′ – A H2′	3.03	<3.5			

The α and ζ angles, which showed the largest spread in values in Table 7, again display the largest fluctuations. The χ angle of thymine has changed to a lower value, 28° vs 140° averaged over the structures, but still has the SYN conformation.

The ϵ torsion angle has changed a little, too. The value ϵ of is now closer to what is expected on the basis of the coupling constant data. The cyclobutane ring conformation is still *trans-syn*. The ϕ_1 and ϕ_2 differ only slightly from the starting value, the difference can be explained by a larger pucker in the cyclobutane ring.

The distance constraint energy is 14 kJ/mole.nm^{-2} averaged over the 20 ps. This is higher than in the generated models. The largest violations of the virtual bounds during the free dynamics simulation are in the constraints around the glycosidic angles (see Table 9). However, inspection of this table also reveals that the violations are not very severe. One can conclude that the free dynamics run did not change the structure much, although a few details are different.

CONCLUSIONS

On the basis of the 2D NOE data used as constraints in distance geometry calculations the solution structure for the photoproduct of d(TpA) has been obtained. The important structural features of the photoproduct are: 1) the cyclobutane linkage is *trans-syn*; 2) the glycosidic angle for thymidine is SYN and for deoxyadenosine is ANTI; 3) the backbone torsion angles β and γ of deoxyadenosine are in a trans and gauche conformation. This last finding also corresponds perfectly with the coupling constant data obtained for this molecule. These structural aspects do not change significantly during the free molecular dynamics run of the photoproduct of d(TpA) in solution. Since distance geometry and distance bound driven dynamics allow a good search of the conformational space we could also determine the spread in the possible structures: the average r.m.s. deviation is 0.53 Å.

The most striking aspect of these structures is the *trans-syn* cyclobutane linkage and the associated SYN-ANTI glycosidic pattern. In normal duplex B-DNA all the glycosidic angles are ANTI and this would favour *cis-syn* geometry of the cyclobutane ring. Indeed, based on the premise that the nucleobase residues in d(TpA) adopt a stacked conformation in solution akin to their disposition in native DNA, the photoproduct was originally assumed (*14*) to have a *cis-syn* stereochemistry. However, it is clear from inspecting a model of a d(TpA) unit in DNA that if the thymine base is rotated into a SYN conformation about the glycosidic bond it can bring the reactive bonds into closer juxtaposition which should promote photoaddition and result in a product with the observed *trans-syn* structure. The requirement for thymidine residues to adopt a SYN conformation provides a reasonable explanation for the much lower quantum yields for the photoreaction (*13*) in base paired duplexes than in their single stranded counterparts which have more conformational freedom.

Detailed structural analyses by NMR spectroscopy have also been carried out on cyclobutane photoproducts with *trans-syn* stereochemistry which were obtained by acetophenone-sensitized irradiation of TpT and TpdC (*3,5*). With these pyrimidine dideoxynucleoside monophosphates, however, the predominant photoproducts have the *cis-syn* stereochemistry and the *trans-syn* isomers respresent a relatively minor species. This contrasts with the behavior of d(TpA) which is shown by HPLC analysis to undergo quite specific conversion into the *trans-syn* photoproduct on UV irradiation in solution.

REFERENCES

1. Wang,S.Y.,ed.(1976) Photochemistry and Photobiology of Nucleic Acids, Vol.I and II, Academic Press, New York
2. Hruska,F.E., Wood,D.J., Ogilvie,K.K. and Charlton,J.L.(1975) Can. J. Chem. 53, 1193–1203
3. Lui,F.T. and Yang,N.C.(1978) Biochemistry 17, 4865–48766.
4. Rycyna, R.E. and Alderfer,J.L.(1985) Nucl. Acids Res. 13, 5949–5963
5. Kemmink,J., Boelens,R. and Kaptein,R.(1987) Eur. Biophys. J. 14, 293–299
6. Kemmink,J., Boelens,R., Koning,T.M.G., Kaptein,R., van der Marel,G.A. and van Boom,J.H.(1987) Eur. J. Biochem. 162, 37–43
7. Kan,L.S., Voituriez,L. and Cadet,J.(1988) Biochemistry 27, 5796–5803
8. Rycyna,R.E., Wallace,J.C., Sharma,M. and Alderfer,J.L.(1988) Biochemistry 27, 3152–3163
9. Taylor,J.S., Garrett,D.S. amd Wang.M.J.(1988) Biopolymers 27, 1571–1593
10. Taylor,J.S., Garrett,D.S. and Cohrs,M.P.(1988) Biochemistry 27, 7206–7215
11. Pörschke,D.(1973) Proc. Nat. Acad. Sci. USA 70, 2683–2686
12. Kumar,S., Sharma,N.D., Davies,R.J.H., Phillipson,D.W. and McCloskey,J.A.(1987) Nucl. Acids Res. 15, 1199–1216
13. Bose,S.N., Davies,R.J.H., Sethi,S.K. and McCloskey,J.A.(1983) Science 220, 723–725
14. Bose,S.N., Davies,R.J.H., Sethi.S.K. and McCloskey,J.A.(1984) Nucl. Acids Res. 12, 7929–7947
15. Shaka,A.J., Keeler,J. and Freeman,R.(1983) J. Magn. Res. 53, 313–340
16. Aue,W.P., Bartholdi,E. and Ernst,R.R.(1976) J. Chem. Phys. 64, 2229–2246
17. Scheek,R.M., Russo,N.,Boelens,R. and Kaptein,R.(1983) J. Am. Chem. Soc. 105, 2914–2916
18. Haasnoot,C.A.G., de Leeuw,F.A.A.M., de Leeuw,H.P.M. and Altona,C. (1980) Tetrahedron Lett. 36, 2783–2792
19. Haasnoot,C.A.G., de Leeuw,F.A.A.M., de Leeuw,H.P.M. and Altona,C.(1980) Org. Magn. Res. 15, 43–52
20. Havel,T.F., Kuntz,I.D. and Crippen,G.M.(1983) Bull. Math. Biol. 45, 665–720
21. Scheek,R.M. and Kaptein,R.(1988) in 'Methods in Enzymology', in press
22. Kaptein,R., Zuiderweg,E.R.P, Scheek,R.M., Boelens,R. and van Gunsteren,W.F. (1985) J. Mol. Biol. 182, 179–182
23. van Gunsteren,W.F., Boelens,R., Kaptein,R., Scheek,R.M. and Zuiderweg,E.R.P (1985) in 'Molecular Dynamics and Protein Structure', Hermans,J., ed. Polycristal Book Service, Western Springs, U.S.A., 92–99

24. Cheng,D.M. and Sarma,R.H.(1977) J. Am. Chem. Soc. 99, 7333–7348
25. Giessner-Prettre,C. and Pullman, B.(1977) J. Mol. Biol. 65, 171–188
26. Altona,C.(1982) Recl. Trav. Chim. Pays Bas 101, 413–433
27. Lankhorst,P.P, Haasnoot,C.A.G., Erkelens,C. and Altona,C.(1984) J. Biomol. Struc. Dyn. 1, 1387–1405
28. Saenger,W.(1984) in 'Principles of Nucleic Acid Structure' Cantor,C.R. ed., pp 9–28, Springer Verlag, New York, 9–28
29. Cadet,J., Voituriez,L., Hruska,F.E. and Grand,A.(1985) Biopolymers 24, 897–903